Video Article

Modeling Astrocytoma Pathogenesis *In Vitro* and *In Vivo* Using Cortical Astrocytes or Neural Stem Cells from Conditional, Genetically Engineered Mice

Robert S. McNeill[1], Ralf S. Schmid[2], Ryan E. Bash[3], Mark Vitucci[4], Kristen K. White[1], Andrea M. Werneke[3], Brian H. Constance[5], Byron Huff[6], C. Ryan Miller[2,3,7]

[1]Department of Pathology and Laboratory Medicine, University of North Carolina School of Medicine

[2]Lineberger Comprehensive Cancer Center, University of North Carolina School of Medicine

[3]Division of Neuropathology, Department of Pathology and Laboratory Medicine, University of North Carolina School of Medicine

[4]Curriculum in Genetics and Molecular Biology, University of North Carolina School of Medicine

[5]Biological and Biomedical Sciences Program, University of North Carolina School of Medicine

[6]Department of Radiation Oncology, Emory University School of Medicine

[7]Department of Neurology, Neurosciences Center, University of North Carolina School of Medicine

Correspondence to: C. Ryan Miller at rmiller@med.unc.edu

URL: http://www.jove.com/video/51763
DOI: doi:10.3791/51763

Keywords: Neuroscience, Issue 90, astrocytoma, cortical astrocytes, genetically engineered mice, glioblastoma, neural stem cells, orthotopic allograft

Date Published: 8/12/2014

Citation: McNeill, R.S., Schmid, R.S., Bash, R.E., Vitucci, M., White, K.K., Werneke, A.M., Constance, B.H., Huff, B., Miller, C.R. Modeling Astrocytoma Pathogenesis *In Vitro* and *In Vivo* Using Cortical Astrocytes or Neural Stem Cells from Conditional, Genetically Engineered Mice. *J. Vis. Exp.* (90), e51763, doi:10.3791/51763 (2014).

Abstract

Current astrocytoma models are limited in their ability to define the roles of oncogenic mutations in specific brain cell types during disease pathogenesis and their utility for preclinical drug development. In order to design a better model system for these applications, phenotypically wild-type cortical astrocytes and neural stem cells (NSC) from conditional, genetically engineered mice (GEM) that harbor various combinations of floxed oncogenic alleles were harvested and grown in culture. Genetic recombination was induced *in vitro* using adenoviral Cre-mediated recombination, resulting in expression of mutated oncogenes and deletion of tumor suppressor genes. The phenotypic consequences of these mutations were defined by measuring proliferation, transformation, and drug response *in vitro*. Orthotopic allograft models, whereby transformed cells are stereotactically injected into the brains of immune-competent, syngeneic littermates, were developed to define the role of oncogenic mutations and cell type on tumorigenesis *in vivo*. Unlike most established human glioblastoma cell line xenografts, injection of transformed GEM-derived cortical astrocytes into the brains of immune-competent littermates produced astrocytomas, including the most aggressive subtype, glioblastoma, that recapitulated the histopathological hallmarks of human astrocytomas, including diffuse invasion of normal brain parenchyma. Bioluminescence imaging of orthotopic allografts from transformed astrocytes engineered to express luciferase was utilized to monitor *in vivo* tumor growth over time. Thus, astrocytoma models using astrocytes and NSC harvested from GEM with conditional oncogenic alleles provide an integrated system to study the genetics and cell biology of astrocytoma pathogenesis *in vitro* and *in vivo* and may be useful in preclinical drug development for these devastating diseases.

Video Link

The video component of this article can be found at http://www.jove.com/video/51763/

Introduction

Astrocytomas are the most common primary brain tumor and glioblastoma (GBM), a grade IV astrocytoma, is the most common and aggressive subtype with a median survival of 12-15 months[1,2]. Invasion of diffuse astrocytomas, particularly GBM, precludes complete surgical resection, limits the effectiveness of adjuvant therapies, and inevitably leads to post-treatment recurrence[3]. Patients initially present either with de novo (primary) GBM or with lower grade astrocytomas that inevitably progresses to (secondary) GBM[4]. GBM is genomically heterogeneous and characterized by mutually exclusive and co-occurring mutations in genes that govern three core signaling pathways: the G_1/S (Rb) cell cycle checkpoint, receptor tyrosine kinase (RTK), and *TP53* pathways[5-7]. GBM consists of four genomic subtypes with distinct expression profiles that resemble different brain cell types, suggesting that GBM subtype is influenced by its cell of origin[6,8,9]. Better astrocytoma models are required to define the role of specific combinations of mutations in particular cell types during astrocytoma pathogenesis. Leveraging these models for more efficient preclinical drug development will ultimately help improve patient outcomes. Current astrocytoma models include established human cell lines, patient derived xenografts (PDX), genetically modified normal human astrocytes and neural stem cells (NSC), and genetically engineered mice (GEM)[10-14]. We developed an alternative, non-germline GEM (nGEM) model[15] utilizing primary brain cells – cortical astrocytes and NSC – harvested from GEM harboring various combinations of floxed oncogenic alleles. The goal was to generate astrocytoma models with genetically

defined cells that could be phenotypically characterized both *in vitro* and *in vivo* and potentially utilized for preclinical drug development in immune-competent mice.

Established human cell lines are the most commonly used model of astrocytoma pathogenesis and drug response *in vitro* and *in vivo.* They are technically straight forward, widely available, and have defined kinetics and tumorigenicity upon orthotopic xenografting in immunodeficient mice[10,11,16-18]. Their disadvantages include the inability to generate established cell lines from low-grade astrocytomas, limiting study only to high-grade astrocytomas; lack of a defined cell of origin; the presence of complex genomic abnormalities, often with genomic profiles that differ markedly from the original patient sample; and susceptibility to phenotypic and genotypic drift during serial culture in serum[11,17,19-22]. The phenotypic consequences of individual oncogenic mutations in established human GBM cell lines can be masked by the multitude of abnormalities that are actually present, which often precludes elucidation of direct genotype-phenotype consequences.

PDX are generated through subcutaneous passage of patient-isolated astrocytoma cells in immunodeficient mice or through their culture as non-adherent spheroids in defined, serum-free medium prior to orthotopic injection into the brains of immunodeficient mice[12,23]. PDX more accurately maintain the genomic landscape of human astrocytomas, but similar to established human cell lines, the phenotypic effect of individual oncogenic mutations can be masked due to their genomic complexity[19,24]. To define the phenotypic consequences of specific oncogenic mutations, particularly in response to novel therapies, panels of established human cell lines or PDX are frequently utilized to establish genotype-phenotype correlations, show generalizability, and minimize the likelihood of cell line-specific effects. While PDX accurately recapitulate the histopathological hallmarks of human astrocytomas, including invasion, orthotopic xenografts of established human cell lines generally do not[21,23,25]. Additionally, normal human astrocytes and NSC have been genetically-engineered with defined oncogenic mutations to model astrocytoma tumorigenesis *in vitro* and *in vivo*[13,14,26]. These cells lack the genomic complexity of established human cell lines and PDX and accurately recapitulate human astrocytoma histopathology, but require xenografting in immunodeficient rodents *in vivo*. Because all human cell models require immunodeficient rodent hosts to prevent immune-mediated xenograft rejection, these models fail to recapitulate the native tumor-stroma interactions of a syngeneic system and lack an intact immune system, limiting preclinical investigation of stroma-targeted and immune-modulatory therapies[10,11].

GEM permit examination of the phenotypic consequences of predetermined combinations of oncogenic mutations *in vivo* during *in situ* tumorigenesis. Whereas non-conditional GEM have mutations within all tissues throughout development, conditional GEM have floxed oncogenic alleles that enable targeting of mutations by restricting Cre-mediated recombination to specific cell types through use of cell type-specific promoters[10,11,15,18]. Conditional astrocytoma GEM have been utilized to elucidate the functional roles of oncogenic mutations in distinct cell types within an intact brain[11]. The preclinical utility of *in situ* gliomagenesis using conditional GEM is limited by a number of factors including 1) the lack of an *in vitro* correlate, 2) difficulty in generating large cohorts of mice with complex genotypes, 3) long latency of *in situ* tumor development, 4) and stochastic tumor progression. Because *in situ* tumorigenesis lacks a corresponding *in vitro* model, drug testing *in vitro* cannot be performed with conventional conditional GEM models. In contrast to other cancers, conditional GEM models of astrocytomas are rarely induced by single oncogenic mutations[11]. Thus, complex breeding schemes are required to generate conditional GEM with multiple oncogenic mutations. Moreover, astrocytoma initiation occurs with variable penetrance after a long latency period in these models, while progression to high-grade astrocytomas generally occurs in a non-uniform, stochastic manner and ultimately gives rise to tumors with complex genomic landscapes and rapid growth kinetics[27,28]. The variable penetrance and stochastic nature of malignant progression in conditional GEM models requires that individual mice be screened by radiographic imaging to detect the presence and location of high-grade astrocytomas before their enrollment in preclinical drug trials. Taken together, these limitations hinder the generation and testing of the large cohorts of conditional GEM required for preclinical drug testing.

The RCAS-tva GEM system, which utilizes avian retroviral (RCAS) vectors to infect GEM engineered to express the viral receptor (tva) on specific neural cell types, has been extensively utilized to model astrocytoma tumorigenesis[11]. In contrast to conditional GEM, this model system enables introduction of multiple oncogenic mutations in specific cells types without the requirement for complex breeding schemes. However, it is limited by variable penetrance, the requirement for actively dividing cells to achieve viral integration, and the random insertion of transgenes into the host genome[29].

Non-germline GEM (nGEM) models, which utilize cells harvested from GEM, are becoming increasingly important because they overcome many of the limitations of other model systems[15]. The role of initiating cell type and co-occurring mutations in astrocytoma pathogenesis are difficult to determine using established human GBM cell lines or PDX because they are derived from end-stage tumors that have accumulated extensive genetic mutations in undefined cell types during the course of malignant progression. In contrast, all grades of astrocytomas can be modeled using nGEM by inducing defined genetic mutations within specific purified brain cell types[11,30]. Thus, the influence of specific genetic mutations and cell type on cellular and molecular phenotypes can be determined *in vitro* and *in vivo*. Similar to established human GBM cell lines, initial *in vitro* drug testing using nGEM can be used to prioritize drugs for *in vivo* testing utilizing the same cells. Tumorigenesis *in vivo* can then be determined by allografting nGEM cells orthotopically into the brains of immune-competent syngeneic littermates[30]. These orthotopic allograft models therefore permit *in vivo* testing not only of conventional cytotoxic and targeted therapies, but immune-modulatory and stroma-targeted therapies as well. Finally, the role of the microenvironment on tumor initiation and progression can be determined by comparing results between nGEM and conventional GEM models using the same mutations in the same cell types.

We and others have developed astrocytoma nGEM using primary cells - astrocytes, NSC, or oligodendrocyte precursor cells (OPC) - harvested from GEM[30-34]. The rationale behind the development of an astrocytoma nGEM was to create a model to determine the phenotypic consequences of oncogenic mutations in specific cell types that could potentially be used for preclinical drug testing *in vitro* and *in vivo* in immune-competent animals. We harvested phenotypically WT cortical astrocytes and NSC from non-Cre expressing, conditional GEM maintained on a >94% C57/Bl6 background with floxed RB pathway - $Rb1^{loxP/loxP}$, or $TgGZT_{121}$ – and floxed RTK/RAS/PI3K pathway - $Nf1^{loxP/loxP}$, $Kras^{G12D}$, $Pten^{loxP/loxP}$ – genes in various combinations[35-39]. We induced genetic recombination *in vitro* using adenoviral vectors encoding Cre recombinase. Because cortical astrocyte harvests contain a mixture of cell types, we used Ad5GFAPCre vectors or dominant oncogenic transgenes, such as $TgGZT_{121}$ driven from the human GFAP promoter, to enrich for $GFAP^+$ cortical astrocytes in these cultures. We defined the phenotypic consequences of G_1/S (Rb), MAPK, and PI3K pathway mutations in cortical astrocytes and NSC *in vitro* and *in vivo*. MAPK and PI3K pathway-activated G1/S-defective astrocytes molecularly mimicked human proneural GBM and, upon orthotopic injection, formed tumors in a pre-defined location with uniform growth kinetics, short latencies, and the histopathological hallmarks of human GBM[30]. Longitudinal monitoring of tumor growth *in vivo* aids preclinical drug testing through normalization of treatment cohorts and quantitative analysis of tumor

growth in response to treatment[40]. We determined tumor growth kinetics by longitudinal bioluminescence imaging of mice injected with luciferase expressing cortical astrocytes. Therefore, cortical astrocytes and NSC derived from conditional GEM provide a tractable model system for definition of functional consequences of astrocytoma-associated mutations and a potential model system for preclinical drug development.

Protocol

All animal studies were approved by the University of North Carolina Institutional Animal Care and Use Committee.

1. Culturing Cortical Astrocytes from Neonatal Mice

1. Preparation
    1. Crumple 2-3 delicate task tissues and place into the bottom of a flask containing 70% ethanol. Place dissecting scissors, curved forceps and 2 pairs of straight micro forceps into this flask. The tissues are used to avoid bending the micro forceps.
    2. Add 1 ml of HBSS to a 60 mm tissue culture dish. Prepare a separate dish for each animal and maintain dishes on ice.
    3. Anesthetize animals per institutional regulations.
    4. Warm 7 ml of DMEM with 10% fetal bovine serum and 1% penicillin-streptomycin (complete DMEM) for each animal in a 37 °C water bath. NOTE: For 5 mice, steps 1.1.1-1.1.4 will take ~15 min.

2. Tissue Harvest
    1. Sacrifice neonatal mouse (day 1-3) per institutional regulations.
    2. Remove dissecting scissors from ethanol, allow them to drip dry, and make a sagittal cut in the skin over the cranium from the spinal cord to the nose.
    3. Make a cut in the cranium along the sagittal suture, starting from the spinal cord and extending past the olfactory bulbs. Take care to keep the scissor tips near the inner surface of the cranium to minimize brain tissue damage.
    4. Using curved forceps, gently peel each hemisphere of the cranium laterally away from the brain.
    5. Using straight micro forceps, gently pinch away the dorsal portion of each cortical hemisphere and place it into the tissue culture dish containing HBSS. Take care to avoid the cerebellum and olfactory bulb. Do not take any tissue below the corpus callosum.
    6. Using a dissecting microscope and 2 pairs of micro forceps, gently remove the meninges from each cortical hemisphere. Return the tissue culture dish to ice until beginning tissue homogenization.
    7. Repeat steps 1.2.1 through 1.2.6 for each additional animal. NOTE: For 5 mice, steps 1.2.1-1.2.7 will take ~30 min.

3. Tissue Homogenization
    1. Using a clean razor blade, finely dice the cortical hemispheres and move the plate to a tissue culture hood.
    2. Transfer the diced tissue into a sterile 15 ml conical tube. Wash the plate with 1 ml of ice cold HBSS and transfer to the tube containing tissue.
    3. Wait until tissue settles to the bottom of the tube, then carefully remove excess HBSS using a pipette.
    4. Add 2 ml of room temperature trypsin/EDTA. Pipette ~10x with a 1 ml pipette to further dissociate cells.
    5. Incubate the cell suspension at 37 °C for 15 - 20 min. Carefully mix by inversion every 5 min.
    6. Add 3 ml of complete DMEM to inhibit trypsin. Pipette ~10x with a 1 ml pipette to mix the solution.
    7. Centrifuge at 200 x g for 5 min at room temperature.
    8. Remove the supernatant with a 1 ml pipette. Do not aspirate the medium because the pellet may be loose.
    9. Resuspend the pellet in 4 ml of 37 °C complete DMEM. Transfer the cell suspension to a 75 cm screw top tissue culture flask. NOTE: For 5 mice, steps 1.3.1-1.3.9 will take ~50 min.
    10. Approximately 16 hr after astrocyte harvest, wash the flask with 4 ml of 37 °C HBSS, then add 4 ml of 37 °C complete DMEM. Maintain the cortical astrocytes at 37 °C in 5% CO_2. NOTE: The wash step is important for removal of non-adherent cells and debris from the culture dish.
    11. When the culture is ~95% confluent, shake overnight at 37 °C in 5% CO_2, remove the media containing the detached cells, then wash the flask with 4 ml of 37 °C HBSS. Add 4 ml of 37 °C complete DMEM and maintain cells at 37 °C in 5% CO_2. NOTE: This step is important to enrich cultures for cortical astrocytes, as contaminating microglia and oligodendrocyte progenitor cells detach with this procedure and are removed from the culture[41].
    12. Repeat steps 1.3.1-1.3.11 for each animal.

4. Induction of Genetic Recombination
    1. 24 hr after completing step 1.3.11, replace the medium with 2 ml of 37 °C complete DMEM. Add 1 ml of 37 °C SCM containing 1 µl of >10^{10} pfu/ml of Ad5CMVCre or Ad5GFAPCre. Incubate for 6 hr at 32 °C in 5% CO_2.CAUTION: Use BSL2 safety precautions when handling recombinant adenovirus.
    2. Remove the virus containing media and add 37 °C complete DMEM without virus to the cortical astrocytes. CAUTION: Use BSL2 safety precautions when handling recombinant adenoviruses and discard the virus-containing media per institutional regulations. NOTE: For 5 astrocyte cultures, steps 1.4.1 - 1.4.3 will take ~15 min excluding the 6 hr incubation.
    3. Expand cortical astrocyte cultures for *in vitro* and *in vivo* characterization. NOTE: Determine the presence of mutations following Cre-recombination by PCR with primers specific for the recombined gene or by immunoblots for either the specific mutated protein or its signaling consequences. The time required for phenotypic stabilization of cortical astrocyte cultures after Cre-recombination will be dependent on the mutations utilized and must be determined empirically (**Figure 2**).

2. Culturing Neural Stem Cells from Neonatal Mice

1. Preparation

1. Before starting the dissection, prepare 4 ml digestion solution per brain by adding 3.1 mg papain and 1.3 mg cysteine to 4 ml dissociation medium - 98 mM Na_2SO_4, 30 mM K_2SO_4, 5.8 mM $MgCl_2$, 0.25 mM $CaCl_2$, 1 mM HEPES (from 1 M HEPES pH 7.4 stock) 20 mM glucose, 0.001% Phenol red, and 0.125 mM NaOH. Addition of papain and cysteine to the dissociation medium will turn the solution yellow.
2. Incubate in 37 °C water bath for 15 min. Mix periodically by inversion.
3. Add 0.1 M NaOH drop wise until digestion solution returns to light red color.
4. In a tissue culture hood, sterile filter the digestion solution using a syringe filter (0.22 µm pore size). Keep the digestion solution on ice.
5. Prepare 50 ml of Stem Cell Medium (SCM) by mixing 44.5 ml NSC Basal Medium, 5 ml NSC supplement, 0.5 ml penicillin-streptomycin, 50 µl 0.2% heparin, 10 µl 100 µg/ml EGF, and 10 µl 100 µg/ml bFGF. SCM is stable for 1 week when stored at 4 °C.
6. Prepare complete HBSS (cHBSS) by mixing 50 ml of 10x HBSS, 1.25 ml 1 M HEPES (pH 7.4), 15 ml 1 M D-glucose, 5 ml 100 mM $CaCl_2$, 5 ml 100 mM $MgSO_4$, and 2 ml 1 M $NaHCO_3$. Bring the total volume to 500 ml with ddH_2O.
7. Filter sterilize cHBSS with a 0.2 µm pore size filter and store at 4 °C.
8. Crumple 2-3 delicate task tissues and place into the bottom of a flask containing 70% ethanol. Place dissecting scissors, curved forceps, and 2 pairs of straight micro forceps into this flask. The tissues are used to avoid bending the micro forceps. NOTE: For 5 mice, steps 2.1.1-2.1.8 will take ~45 min.

2. Tissue Harvest
   1. Sacrifice neonatal (day 1-3) mice per institutional regulations.
   2. Remove dissecting scissors from the 70% ethanol, allow them to drip dry, and make a sagittal cut in the skin over the cranium from the spinal cord to the nose.
   3. Make a cut in the cranium along the sagittal suture, starting from the spinal cord and extending past the olfactory bulbs. Take care to keep the scissor tips near the inner surface of the cranium to minimize brain tissue damage.
   4. Using curved forceps, gently peel each hemisphere of the cranium laterally away from the brain.
   5. Gently remove the entire brain and place in ice cold cHBSS.
   6. Using a dissection microscope, carefully remove meninges from the brain with fine dissection tools.
   7. Place the brain on its bottom surface and remove cerebellum/hindbrain and olfactory bulb/frontal cortex with vertical (coronal) cuts with a size 11 scalpel.
   8. Rotate the remaining brain by 90° to place it on the caudal portion, thus generating a coronal view of the brain. Locate the lateral ventricles.
   9. Cut out a cubical section containing the subventricular zone (SVZ).
   10. Transfer SVZ-containing tissue to a 60 mm tissue culture dish with fresh ice cold cHBSS and mince tissue with size 11 scalpel.
   11. Transfer the minced tissue into a sterile 15 ml tube. Place the tube on ice.
   12. Wash the petri dish with 1-2 ml ice cold cHBSS. Transfer the wash solution to the tube containing tissue.
   13. Repeat steps 2.2.1-2.2.12 with additional neonatal mice if necessary. Transfer all 15 ml tubes to a tissue culture hood for the remainder of the protocol. NOTE: For 5 mice, steps 2.2.1 - 2.2.13 will take ~45 min.

3. Tissue Homogenization
   1. Place the digestion solution (prepared in step 2.1.1) in a 37 °C water bath for 5 min. Also, warm 2 ml SCM per brain in a 37 °C water bath.
   2. Carefully remove the supernatant of the minced tissue with a 1 ml pipette. Do not aspirate.
   3. Add 2 ml 37 °C digestion solution per 15 ml tube and mix carefully by inversion.
   4. Incubate in 37 °C water bath for 15 min. Mix by inversion every 5 min.
   5. Add another 2 ml of 37 °C digestion solution to each tube and repeat step 2.3.4.
   6. Allow the cells to settle to the bottom of the tube by gravity, then remove the supernatant from digested tissue using a 1 ml pipette.
   7. Add 2 ml of 10 µM E-64 diluted in cHBSS and mix carefully by inversion.
   8. Incubate for 3 min at room temperature.
   9. Allow the cells to settle to the bottom of the tube by gravity, then remove the supernatant from digested tissue.
   10. Add 1 ml of 37 °C cHBSS and homogenize with a 1 ml pipette tip (~20 strokes). Avoid injecting air bubbles during tissue homogenization.
   11. Pass the tissue homogenate through a 40 µm pore size cell strainer, then rinse the strainer with 5 ml of 37 °C cHBSS.
   12. Centrifuge the tissue homogenate at 125 x g for 5 min.
   13. Remove 95% of supernatant with a 1 ml pipette without disturbing the cell pellet. Carefully resuspend cell pellet in 200 µl 37 °C SCM with a 200 µl pipette tip.
   14. Add 1.8 ml 37 °C SCM and transfer the cell suspension to a well of a sterile 6 well plate. NOTE: For 5 mice, steps 2.3.1-2.3.14 will take ~75 min.

4. Neural Stem Cell Culture
   1. Replenish the medium after 3 days by adding another 2 ml 37 °C SCM.
   2. After 7 days, transfer the neurospheres to a 15 ml tube and let the neurospheres settle by gravity for >5 min.
   3. Remove the supernatant and add 2 ml 37 °C SCM.
   4. Transfer the neurospheres to a new well of a 6 well plate.
   5. Add 2 ml of 37 °C SCM every 3-4 days, and change medium completely every 7 days.
   6. If neurospheres are > 100 µm in diameter, carefully dissociate with stem cell dissociation solution and replate the NSC at the desired cell density.

5. Induction of Genetic Recombination
   1. Add 1 ml of 37 °C SCM containing 1 µl of $>10^{10}$ pfu/ml of Ad5CMVCre or Ad5GFAPCre to the 2 ml of SCM currently on the cells. CAUTION: Use BSL2 safety precautions when handling recombinant adenovirus.
   2. Incubate for 6 hr at 32 °C in 5% CO_2.
   3. Transfer SCM with neurospheres into a 15 ml tube and let spheres settle by gravity for 5 min.

4. Remove the supernatant first with a 1 ml pipette, then with a 200 µl pipette. CAUTION: Use BSL2 safety precautions when handling recombinant adenoviruses and discard the virus-containing media per institutional regulations.
5. Add 2 ml of 37 °C SCM without virus to the NSC, then transfer to a 6 well plate. NOTE: For 5 NSC cultures, steps 2.5.1-2.5.5 will take ~15 min excluding the 6 hr incubation.
6. The next day, repeat steps 2.5.1-2.5.5, followed by neurosphere passaging when necessary. The spheres can now be expanded for 2-3 passages before *in vitro* characterization and orthotopic injection in mouse brains *in vivo*. NOTE: Determine the presence of mutations following Cre-recombination by PCR with primers specific for the recombined gene or by immunoblots for either the specific mutated protein or its signaling consequences. The time required for phenotypic stabilization of NSC cultures after Cre-recombination will be dependent on the mutations utilized and must be determined empirically (**Figures 2** and **3**).

3. Orthotopic Injection of Recombined Cells into the Brain of Recipient Iimmunocompetent Mice

1. Preparation of 5% Methyl Cellulose
    1. Dissolve 5 g of 15 cPs methyl cellulose in deionized water to a final volume of 50 ml in a 100 ml screw cap bottle. Add the powder slowly while stirring at 4 °C to prevent clumping. It can take up to 24 hr of stirring at 4 °C for all the methyl cellulose to enter solution.
    2. Weigh the bottle and record the weight.
    3. Autoclave the 5% methyl cellulose solution. Once autoclaved, the methyl cellulose will become a semisolid gel.
    4. Weigh the bottle and calculate the weight lost during autoclaving.
    5. Aseptically add 1 ml of sterile water for every gram of weight lost.
    6. Place on ice and add 50 ml of ice cold 2x DMEM.
    7. Mix overnight using a magnetic stirrer at 4 °C. Use sterile technique to divide the 5% methyl cellulose solution into 20 ml aliquots. Store aliquots at 4 °C for up to six months or until the 2x DMEM expires. NOTE: Preparation of 5% methyl cellulose solution in steps 3.1.1-3.1.7 will take ~2.5 days.

2. Preparation of Cortical Astrocytes for Injection
    1. Harvest cortical astrocytes when ~90% confluent.
    2. To harvest, aspirate complete DMEM and wash plates with an equal volume of 37 °C HBSS.
    3. Add enough trypsin to cover the plate. Gently tilt and tap the plate until cells start to detach.
    4. Inactivate trypsin with an equal volume of 37 °C complete DMEM.
    5. Transfer cells to a 50 ml conical tube and wash the plate with the same volume of 37 °C complete DMEM used in 3.2.4.
    6. Transfer wash media to the tube containing cells. Centrifuge at 200 x g for 3 min.
    7. Aspirate supernatant and resuspend cells in 1 ml of 37 °C complete DMEM.
    8. Count the cell suspension using a hemocytometer or another appropriate cell counter to determine number of cells/µl.
    9. Transfer the desired number of cells to a new 15 ml conical tube. Centrifuge at 200 x g for 3 min.
    10. Resuspend cells in 800 µl of 37 °C complete DMEM. Determine the volume of the cell pellet (total volume of cell suspension – 800 µl). NOTE: It is essential to achieve an accurate cell concentration for injection. Thus, the volume of the cell pellet must be determined in this step in order to calculate the volume of 5% methyl cellulose to add in step 3.2.12.
    11. Transfer cells to a sterile 1.5 ml microcentrifuge tube and then centrifuge at 200 x g for 3 min.
    12. Aspirate supernatant from the cell pellet and resuspend the cortical astrocytes in the appropriate volume of ice-cold 5% methyl cellulose (desired total volume – volume of the cell pellet) to obtain the desired number of cells/µl.
    13. Place cells on ice until injection.
    14. Place a 250 µl glass syringe into a Repeating Antigen Dispenser then place a blunt 18 G needle onto the syringe.
    15. Withdraw the plunger slowly with the needle in the cortical astrocyte suspension; there will be an air bubble above the cells that must be removed, since air bubbles will compress and diminish the volume actually injected into the brain.
    16. Hold the tip of the needle just above the cortical astrocyte suspension and push the plunger in quickly. The air bubble will move faster than the cell suspension and will be mostly expelled.
    17. Repeat step 3.2.16 until all air bubbles are removed from the needle.
    18. Fill the syringe to about ~200 µl, then hold the needle up and pull the plunger back until it stops. Little air bubbles can be removed by holding the needle tip up and rapidly pushing the plunger in about 50 µl then slowly withdrawing to full capacity.
    19. Keep the tip upright and repeat step 3.2.18 4-5x.
    20. Discard the 18 gauge needle and fit a 27 G needle onto the syringe.
    21. Press the button on the antigen dispenser until fluid is expelled from the needle. NOTE: For 1 astrocyte cell line, steps 3.2.1-3.2.21 will take ~60 min.

3. Preparation of NSC for Injection
    1. When neurospheres are > 100 µm in diameter, transfer to 15 ml tubes and let the neurospheres settle by gravity for >5 min.
    2. Remove the supernatant and dissociate the neurospheres with a gentle dissociation reagent, such as stem cell dissociation solution or accutase according to the manufacturer's instructions or with %0.05 trypsin-EDTA as described[42].
    3. Inhibit the dissociation reagents according to the manufacturer's instructions without exposing the NSC to serum. Centrifuge at 100 x g for 5 min.
    4. Aspirate supernatant, then resuspend the cells in 1 ml of 37 °C cHBSS to generate a single cell suspension.
    5. Count the cells using a hemocytometer or another appropriate cell counter to determine the number of cells/µl.
    6. Transfer the desired number of NSC to a new 15 ml conical tube. Centrifuge at 100 x g for 5 min.
    7. Resuspend cells in 800 µl of 37 °C HBSS. Determine the volume of the cell pellet (total volume of cell suspension – 800 µl). NOTE: It is essential to achieve an accurate cell concentration for injection. Thus, the volume of the cell pellet must be determined in this step in order to calculate the volume of 5% methyl cellulose to add in step 3.3.9.
    8. Transfer the cells to a sterile 1.5 ml microcentrifuge tube and then centrifuge at 100 x g for 5 min.

9. Aspirate the supernatant and finish preparing the cells for orthotopic injection as in 3.2.12-3.2.21. NOTE: For 1 NSC cell line, steps 3.3.1-3.3.9 will take ~60 min.

4. Preparation of Mouse for Injection
    1. Anesthetize the recipient animal via a I.P. injection of 250 mg/kg Avertin (2,2,2 Tribromoethanol) or 100 mg/kg ketamine plus 10 mg/kg xylazine, per institutional IACUC guidelines. NOTE: Utilized herein are mice at 3-6 months of age as allograft hosts. Mice at different ages may be utilized to investigate the microenvironmental impact of developmental brain age on tumorigenesis.
    2. Shave the scalp over the incision site with clippers or scissors.
    3. Sterilize the surgical site with 3 alternating swabs of 70% ethanol and betadine.
    4. Apply ophthalmic ointment to the eyes to prevent any damage due to loss of blink reflex.
    5. Assess depth of anesthesia by pedal withdrawal (toe pinch) reflex. NOTE: For 5 mice, steps 3.4.1-3.4.5 will take ~15 min.

5. Orthotopic Implantation
    1. Secure the animal in the stereotaxic frame.
    2. Make an incision over the sagittal suture approximately 0.5 cm long between the ears and eyes.
    3. Locate the intersection of the coronal and sagittal sutures (Bregma), as well as the intersection of the lambdoid and sagittal sutures (Lambda). Ensure that Bregma and Lambda are in the same horizontal plane.
    4. Attach the syringe containing the cell suspension and repeating antigen dispenser to the stereotaxic frame over the head. Bring the tip of the 27 G needle into contact with Bregma. This is the origin that will be used for the manipulation of three dimensional coordinates.
    5. Raise the needle slightly off the skull surface and move 2 mm lateral and 1 mm rostral from Bregma.
    6. Lower the needle carefully through the skull to its destination 4 mm ventral from Bregma. NOTE: We utilized these stereotactic coordinates to target the basal ganglia. Different stereotactic coordinates may be utilized to investigate the microenvironmental impact of different brain regions on tumorigenesis.
    7. Inject 5 µl of the cell suspension by activating the repeating antigen dispenser one time. Leave the needle in place for 2 min to allow intracranial pressure to equilibrate.
    8. Withdraw the needle slowly over a period of 30 sec. Use a cotton swab to apply pressure to any bleeding that may occur.
    9. Approximate the wound edges and close the incision using tissue adhesive. Administer 20 µl of Lidocaine subcutaneously at the incision site. NOTE: For 5 mice, steps 3.5.1-3.5.9 will take ~50 min. The UNC IACUC approved the postoperative use of local anesthesia only. Consultation with local institutional IACUC is recommended regarding requirements for postoperative analgesic use after this procedure.

6. Post-Surgical Care
    1. Place the animals in a clean, warm cage to recover. Animals should not be placed directly into bedding, as accidental aspiration may occur.
    2. Observe the animals for resumption of normal behavior such as grooming, eating, and defecation. NOTE: Resumption of normal behavior can take ~60 min.

Representative Results

We developed an nGEM model system with cortical astrocytes and NSC harvested from neonatal GEM harboring floxed conditional oncogenic alleles that can be phenotypically characterized *in vitro* and *in vivo* (**Figure 1**). In order to investigate the consequences of oncogenic mutations specifically in cortical astrocytes *in vitro*, it is critical to first enrich for astrocytes. Cortical astrocyte harvests contain a mixture of microglia, astrocytes, oligodendrocytes, OPC, and neurons, but mechanical and genetic methods can aid in astrocyte enrichment. Whereas neurons die under normal culture conditions, microglia and oligodendrocytes can be removed by shaking overnight[41,43]. Additionally, genetic recombination of floxed, oncogenic alleles targeted to $GFAP^+$ astrocytes using an Ad5GFAPCre can enrich for astrocytes. We used this method to infect cortical harvests from $Rb1^{loxP/loxP}$ GEM pups with floxed $Nf1^{loxP/loxP}$ and/or $Pten^{loxP/loxP}$ alleles. Ad5GFAPCre infection caused a proliferative advantage in the recombined $GFAP^+$ astrocytes, which increased astrocyte purity from 59% to > 90% after 5 - 9 passages in culture (**Figures 2A** and **2B**). Alternatively, we enriched for astrocytes by expressing T_{121} under control of the *GFAP* promoter to induce a proliferative advantage in astrocytes harvested from *TgGZT*$_{121}$ mice (**Figure 2C**). While cortical astrocytes grow adherent to the culture dish (**Figure 2C**), NSC grow as non-adherent neurospheres *in vitro* (**Figure 3A**). Both WT NSC and NSC with recombined, floxed oncogenic alleles – *TgGZT*$_{121}$ (T), *Kras*^{G12D} (R), and homozygous *Pten* deletion ($P^{-/-}$), referred to as $TRP^{-/-}$ – express the NSC marker Sox2, while only NSC harvested from GEM containing *TgGZT*$_{121}$ express T_{121} after Cre-mediated recombination (**Figure 3B**).

To determine how G_1/S (Rb), MAPK and/or PI3K pathway alterations affect growth of $GFAP^+$ astrocytes *in vitro*, proliferation was examined using two methods. MTS and cell counting showed that expression of T_{121} and $Kras^{G12D}$ increased the proliferation of cortical astrocytes (**Figures 4A** and **4B**). Similarly, homozygous *Rb1* (Rb) and *Nf1* (N), deletion combined with heterozygous *Pten* ($P^{+/-}$) deletion also increased cortical astrocyte proliferation (**Figure 4C**). Transformed cells have unlimited proliferative capacity. The transforming effects of mutations can be measured *in vitro* using colony formation assays. We therefore tested the transforming effects of T_{121} and $Kras^{G12D}$ expression and homozygous *Pten* deletion in $TRP^{-/-}$ cortical astrocytes by colony formation assay as previously described[44]. Whereas WT astrocytes did not form colonies, T astrocytes formed colonies at 1.03% efficiency. Notably, $TRP^{-/-}$ astrocytes had the highest colony formation efficiency at 6.40% (**Table 1**). In order to be suitable for preclinical drug testing, it is important that *in vitro* tumor models be easily manipulated genetically. Additional genetic alterations can be stably introduced into cortical astrocytes by plasmid or viral vectors. As an example, we stably transduced the *luciferase* gene into $TRP^{-/-}$ astrocytes ($TRP^{-/-}$ luc) using a VSV-pseudotyped pMSCV retroviral vector. Expression of luciferase increased luminescence ~1,000 fold compared to parental cells (**Figure 4D**). Additionally, GEM-derived cortical astrocytes can be used to determine the efficacy of targeted inhibitors *in vitro*. We have shown previously that treatment with low dose PI-103, a dual mTOR/PI3K inhibitor, inhibited PI3K signaling without affecting cell viability[30]. However, the cytostatic/cytotoxic effects of higher PI-103 doses were not determined. Thus, we tested whether PI-103 can reduce $TRP^{-/-}$ astrocyte growth *in vitro*. PI-103 caused a maximal 88% reduction in $TRP^{-/-}$ astrocyte growth (**Figure 4E)**. We have previously utilized orthotopic allografts of $TRP^{-/-}$ astrocytes to test other clinically relevant therapeutics *in vivo* (Schmid *et al*., manuscript submitted)[45,46]. These data

suggest that transformed cortical astrocytes harvested from conditional GEM may provide a flexible model system in which to perform preclinical drug testing in immune competent mice.

Xenografts of established human cell lines and PDX require immunodeficient hosts. In contrast to PDX, many established human GBM cell lines do not recapitulate the histopathological features of GBM. For example, U87MG orthotopic xenografts formed circumscribed tumors that did not invade normal brain (**Figure 5A**). In contrast, injection of $TRP^{-/-}$ astrocytes into the brains of immune competent, syngeneic mice yielded invasive tumors that recapitulated the histological features of their human counterparts, particularly invasion of normal brain (**Figure 5B**). To longitudinally quantify $TRP^{-/-}$ allograft growth, mice were sacrificed every 5 days after cell injection and tumor burden was determined by quantifying tumor area on H&E-stained brain sections. Tumor area increased exponentially over time (**Figure 5C**). Orthotopic injection of 10^5 $TRP^{-/-}$ astrocytes into recipient brains led to neurological morbidity, with a median survival of 22 days (**Figure 5D**). In addition to cortical astrocytes, we performed orthotopic injections using $TRP^{-/-}$ NSC. $TRP^{-/-}$ NSC-derived tumors were T_{121} positive, proliferative, and maintained expression of the NSC marker Sox2 (**Figure 6**). Of note, injection of cortical astrocytes and NSC harvested from WT C57Bl/6 mice as well as phenotypically WT cortical astrocytes or NSC with unrecombined, floxed oncogenic alleles from conditional GEM failed to elicit tumorigenesis during this time frame (data not shown). Longitudinal imaging *in vivo* has been used to monitor tumor growth kinetics in response to drug treatments[40]. Thus, $TRP^{-/-}$ luc astrocytes were injected into the brains of immune competent syngeneic littermates and tumor growth was determined by serial bioluminescence imaging. Bioluminescence increased 15 fold over 16 days (**Figures 7A** and **7B**). We have demonstrated that cortical astrocytes and NSC harvested from conditional GEM can be genetically modified and phenotypically characterized *in vitro* and *in vivo* for definition of the genetics and cell biology of astrocytoma pathogenesis and potentially used for preclinical drug development.

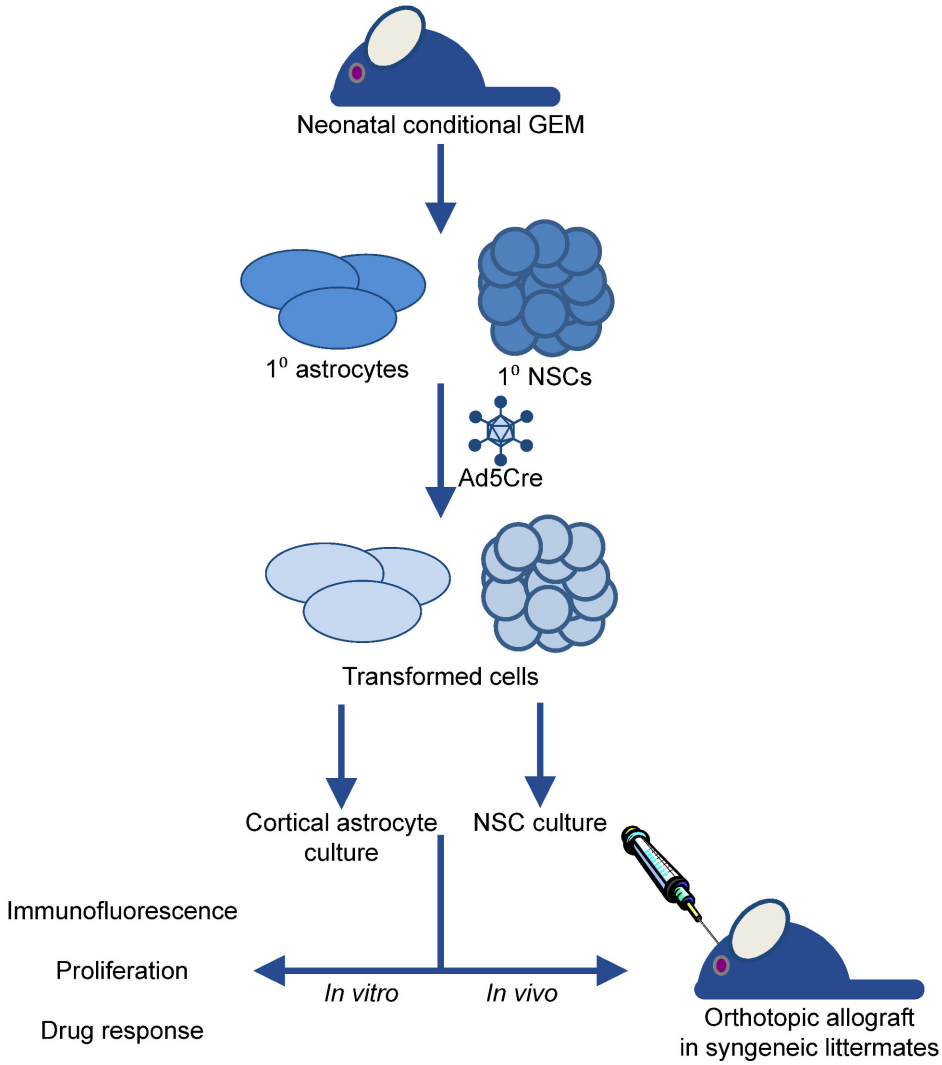

Figure 1. Schematic of cortical astrocyte and NSC harvest from nGEM. Phenotypically WT cortical astrocytes and NSC were harvested from GEM with conditional oncogenic alleles. Genetic recombination was induced *in vitro* with an AdCre vector. Transformed cells were phenotypically characterized *in vitro* by various methods and *in vivo* by orthotopic injection into the brains of immune-competent, syngeneic littermates.

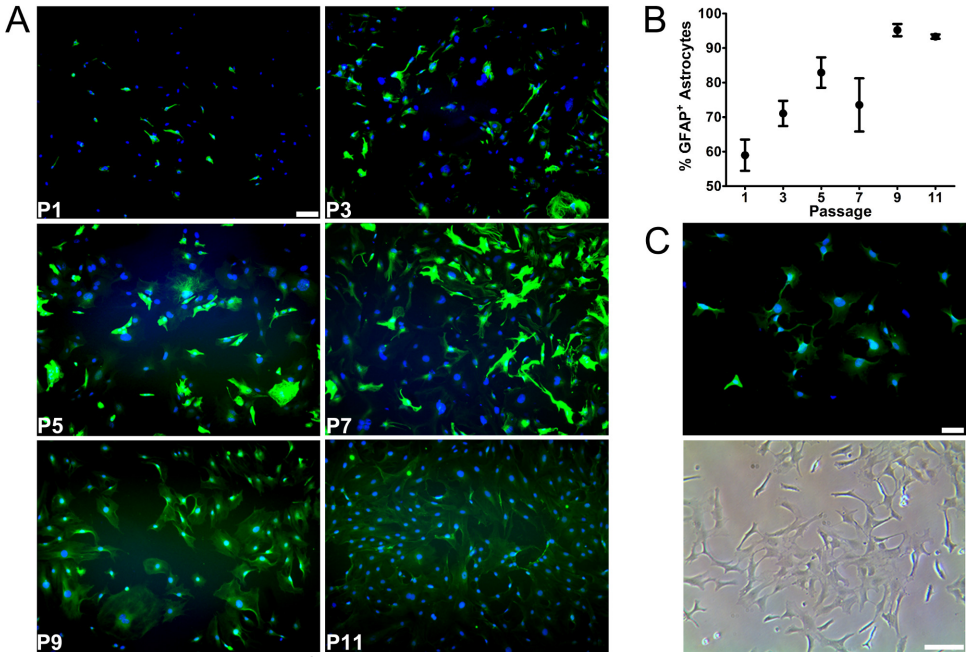

Figure 2. Enrichment of GFAP$^+$ astrocytes upon serial passaging *in vitro*. Representative immunofluorescence images showing GFAP$^+$ astrocytes harvested from Rb1$^{loxP/loxP}$ GEM pups with Nf1$^{loxP/loxP}$ and/or Pten$^{loxP/loxP}$ in which genetic recombination was induced with Ad5GFAPCre and the cells passaged X times (PX) (**A**). Quantification of enrichment of GFAP$^+$ astrocytes in panel A. Bars represent standard error from 3-24 replicates (**B**). Representative immunofluorescence (top) and phase contrast (bottom) images of adherent cortical astrocytes harvested from *TgGZT$_{121}$* GEM pups that express T$_{121}$ from the GFAP promoter at passage 9 after recombination with Ad5CMVCre *in vitro* (**C**). Astrocytes were quantified as the number of GFAP$^+$ (green) cells divided by the total number of DAPI-stained nuclei (blue) at every other passage. Images were taken at 10X original magnification (A,C). Scale bars represent 100 µm (A,C). Please click here to view a larger version of this figure.

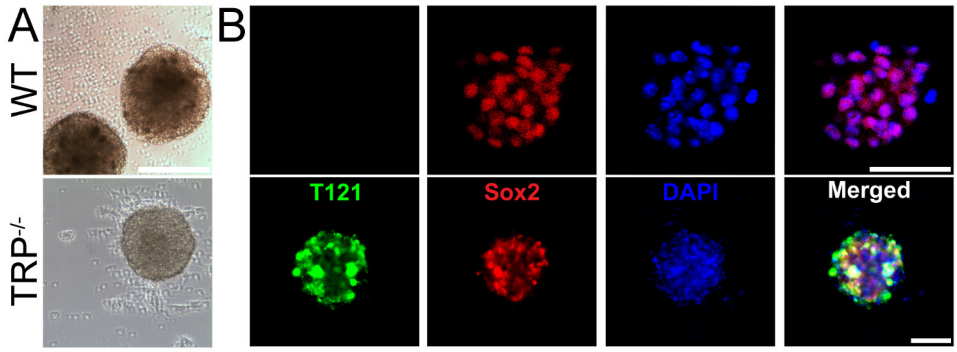

Figure 3. WT and recombined NSC harvested from TRP$^{-/-}$ GEM. Representative phase contrast images of phenotypically WT (top) and TRP$^{-/-}$ (bottom) NSC grown as neurospheres *in vitro* (**A**). Representative immunofluorescence staining for T$_{121}$ (green) and Sox2 (red) expression in WT (top) and TRP$^{-/-}$ (bottom) neurospheres (**B**). Scale bars represent 100 µm (A,B). Please click here to view a larger version of this figure.

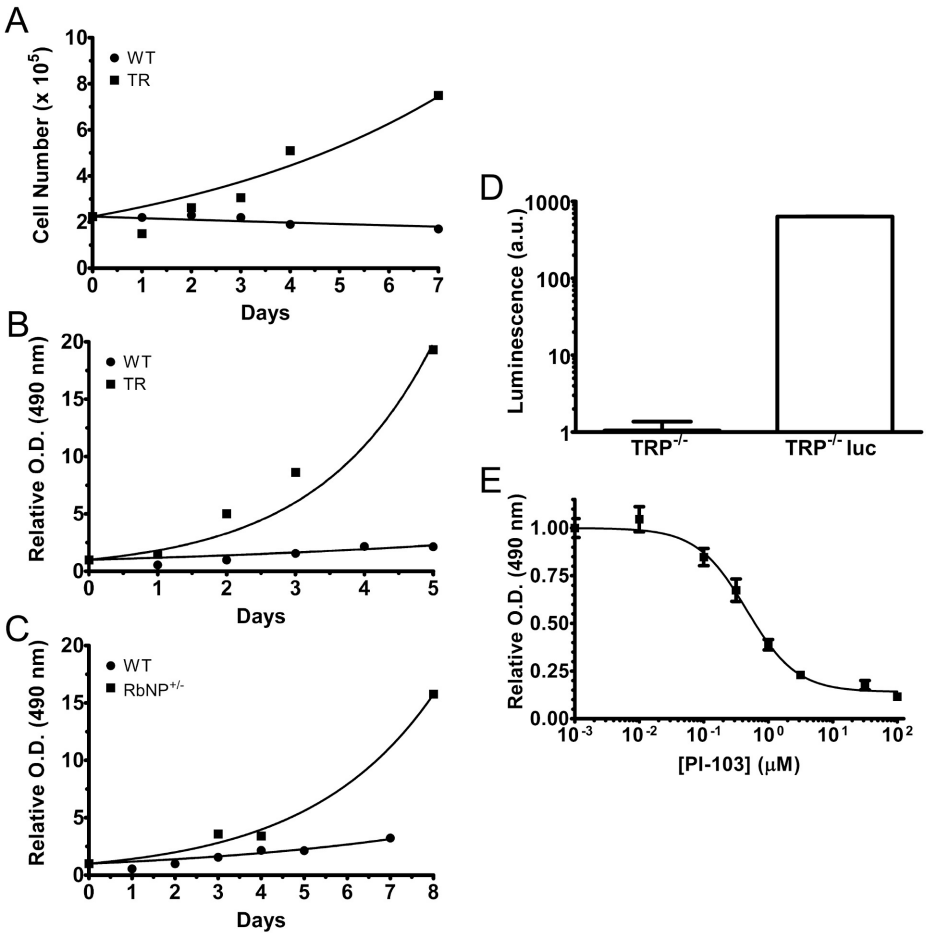

Figure 4. Characterization of cortical astrocytes *in vitro*. Growth of WT and TR cortical astrocytes was determined by counting cells on days 1-7 (**A**). Relative optical density (O.D.) of WT and TR cortical astrocytes was determined by MTS (**B**). Relative growth of WT and recombined $Rb1^{-/-}$;$Nf1^{-/-}$;$Pten^{+/-}$ ($RbNP^{+/-}$) astrocytes was determined by MTS (**C**). Luminescence of parental $TRP^{-/-}$ and luciferase expressing $TRP^{-/-}$ astrocytes ($TRP^{-/-}$ luc) (**D**). Relative O.D. of $TRP^{-/-}$ astrocytes treated with PI103 for 5 days as determined by MTS (**E**). Proliferation and dose response was calculated using the exponential growth equation in GraphPad Prism 5. Bars represent standard error from 6 replicates per condition. Please click here to view a larger version of this figure.

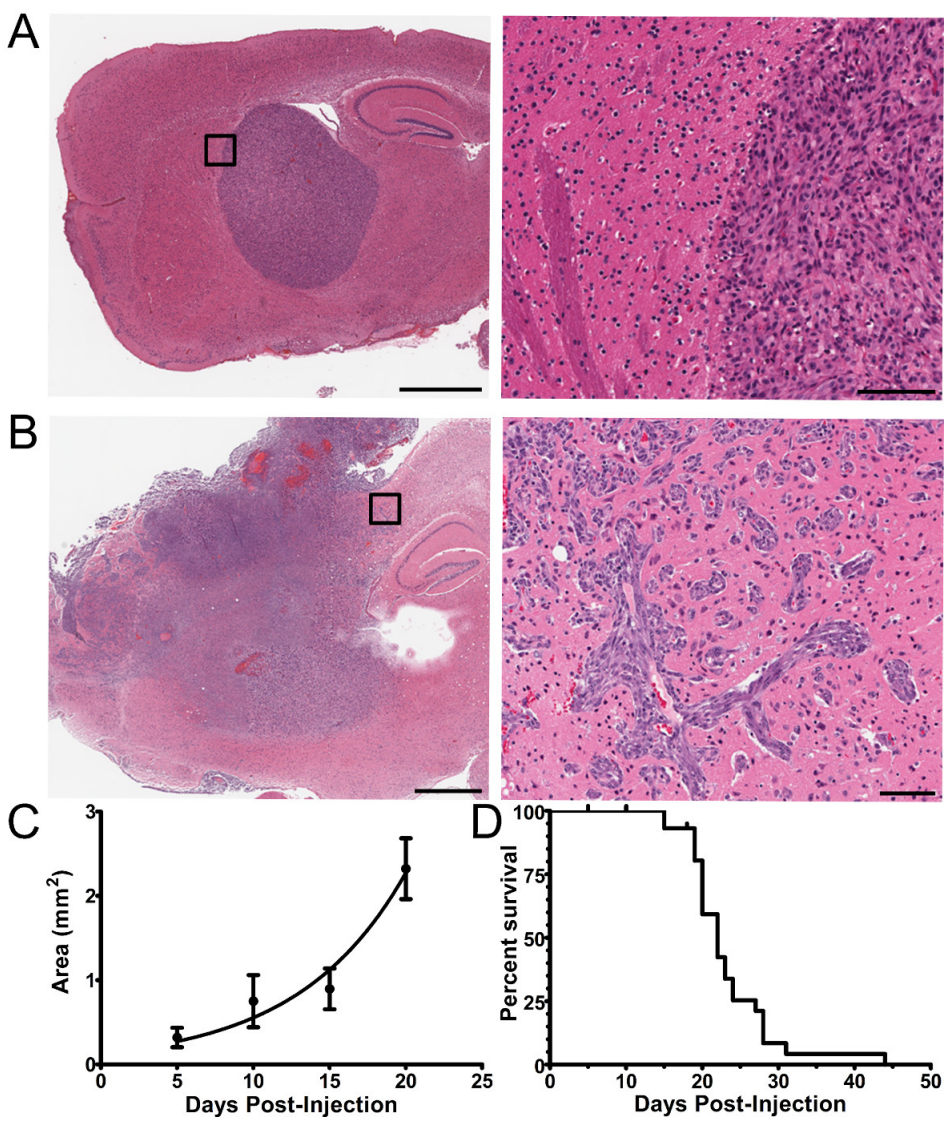

Figure 5. *In vivo* gliomagenesis. Representative H&E stained section of a U87MG xenograft shows discrete tumor margins (**A**). Representative H&E stained section of a $TRP^{-/-}$ allograft shows diffuse invasion of normal brain (**B**). Scale bars in left and right H&E images represent 1 mm and 100 µm, respectively. Tumor area was determined by analyzing H&E stained sections of formalin fixed, paraffin embedded brains from immune-competent, syngeneic littermates injected with 10^5 $TRP^{-/-}$ astrocytes and sacrificed at 5 day intervals post-injection. (**C**). Kaplan–Meier survival analysis of $TRP^{-/-}$ allograft mice aged to morbidity shows a median survival of 22 days (**D**).

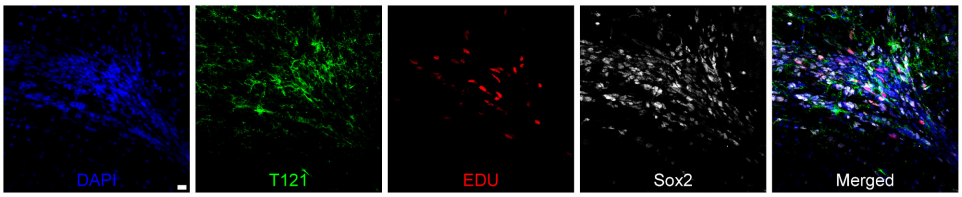

Figure 6. Immunofluorescence of $TRP^{+/-}$ NSC allografts. Representative immunofluorescence images show that $TRP^{+/-}$ NSC injected into the brains of immune-competent, syngeneic littermates express T_{121} (green) and Sox2 (white) and proliferate, as determined by EdU (red) incorporation. Mice were perfused with EdU and sacrificed 6 weeks post-injection and their brains perfused with paraformaldehyde. Scale bar represents 20 µm. Please click here to view a larger version of this figure.

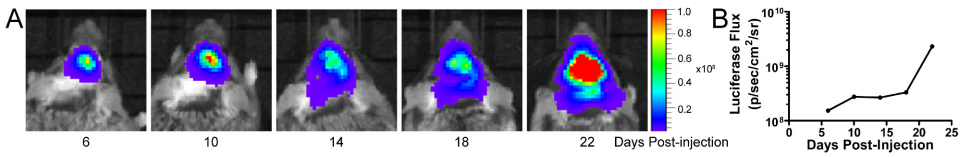

Figure 7. Longitudinal imaging of TRP$^{-/-}$ luc allografts. Representative bioluminescence images (A) and quantification of luciferase flux over time (B) shows growth of TRP$^{-/-}$ allografts in immune-competent, syngeneic mice injected with 10^5 TRP$^{-/-}$ luc cortical astrocytes and imaged at the indicated days post-injection. Please click here to view a larger version of this figure.

Genotype	Plating efficiency (%)	SEM
WT	0	0
T	1.03	0.15
TRP$^{-/-}$	6.40	0.83

Table 1. Colony formation of cortical astrocytes. WT, T and TRP$^{-/-}$ cortical astrocytes were plated in triplicate at 4,000, 2,000, and 250 cells/well respectively. Colonies were stained with crystal violet 14 days after plating, imaged, and counted using ImageJ. Plating efficiency was calculated as the number of colonies divided by the number of cells plated.

Discussion

The most critical steps to ensure proper harvest and culture of cortical astrocytes are 1) to excise the cortex without taking tissue below the corpus callosum, 2) to remove the meninges, 3) to thoroughly dissociate the cells, and 4) to enrich for GFAP$^+$ astrocytes. Although we used mechanical (shaking) and genetic (restriction of genetic recombination with an Ad5GFAPCre vector or utilization of a dominant transforming transgene (*TgGZT$_{121}$*) under *GFAP* promoter control) methods to enrich for GFAP$^+$ astrocytes, other techniques have been utilized to purify cortical astrocytes. For example, contaminating microglia can be removed by treating confluent cultures with a mitotic inhibitor followed by l-leucine methyl ester[47]. The morphology and expression profiles of astrocytes mechanically purified and cultured in serum-containing media differ from acutely isolated astrocytes, with the former hypothesized to represent either more immature astrocytic cells or a reactive astrocyte phenotype[48,49]. More recently, an immunopanning method has been developed to prospectively purify cortical rodent astrocytes and their expression profiles more closely mimicked acutely purified astrocytes when cultured in growth factor-supplemented, serum-free media[49]. The impact of the conventional, mechanical method of cortical astrocyte enrichment and culture versus the more recently developed immunopanning method on the phenotypes investigated herein remain unclear. Regardless of the method utilized, it is essential to enrich for GFAP$^+$ cortical astrocytes to determine the phenotypic consequences of oncogenic mutations specifically within this cell type.

Critical steps for harvesting NSC are 1) to accurately locate the SVZ, 2) to minimize damage to the SVZ during dissection, and 3) to filter the cells following dissociation before plating. Precise NSC dissection technique is necessary to locate and harvest the SVZ. Because NSC grow in suspension culture, it is essential to filter the cell suspension after dissociation to reduce the amount of floating debris. Although we utilized growth in SCM to select for NSC, NSC can be prospectively isolated by fluorescence-activated cell sorting of the SVZ tissue homogenate[50]. After induction of genetic recombination *in vitro*, it is important to monitor the cellular characteristics of the cortical astrocyte and NSC cultures across passages. Because we did not prospectively enrich for astrocytes or NSC during tissue harvest, we serially monitored enrichment and quantified purity of the cell type of interest by immunofluorescence staining with known cell-type specific markers (GFAP for astrocytes, Sox2 for NSC). Additionally, we recommend systematically monitoring the expected signaling consequences of oncogenic mutations both before and at each passage after Cre-mediated recombination by immunoblotting and phenotypically characterizing cells at the earliest passage at which purity is maximized and mutation induced signaling alterations stabilize.

An important consideration in utilizing primary cell cultures is their inherent replicative capacity and the phenotypic impact of the induced mutations. Phenotypically WT murine astrocytes have limited replicative capacity and can only be passaged 3 - 4 times in culture before they undergo replicative senescence[31]. Moreover, many cancer associated mutations, particularly in MAPK pathway genes, cause oncogene-induced senescence *in vitro*[51]. Thus, if the induced mutations fail to immortalize cells and protect them from oncogene-induced senescence, they cannot be serially passaged for phenotypic characterization *in vitro*. Viral oncoproteins such as HPV E6/E7 and SV40 large T antigen have been extensively utilized to immortalize many human and murine cell types in culture, including astrocytes[13,26,30]. We have previously shown that ablation of the G1/S cell cycle checkpoint with T was sufficient to immortalize cortical astrocytes, but not sufficient to cause lethal astrocytomas *in vivo*. In contrast, activation of MAPK and PI3K signaling in TRP$^{-/-}$ astrocytes led to formation of GBM in the orthotopic allograft model system[30]. Thus, the effects of T, R, and P mutations on murine astrocyte transformation *in vitro* as defined by colony formation assays correlated with *in vivo* tumorigenesis in orthotopic allografts.

Like all models that require surgical implantation of tumor cells, orthotopic injection of transformed, nGEM cells into syngeneic mouse brains will elicit an acute wound response, termed reactive gliosis. During this response, neural cells, including astrocytes, oligodendrocyte progenitor (NG2$^+$) glia, and microglia, proliferate and acquire a more primitive differentiation state, largely in response to secreted proteins such as sonic hedgehog[52,53]. However, the proliferative phase of reactive gliosis in response to stab wounding is relatively short, typically one week[53]. We have previously shown that injection of TRP$^{-/-}$ astrocytes efficiently induces tumorigenesis during this time frame, yielding low-grade astrocytomas that frequently progress to high-grade astrocytomas, including GBM. In contrast, injection of T or TP$^{-/-}$ astrocytes infrequently develop into low-grade astrocytomas at 1-3 weeks post-injection and these tumors fail to progress to high-grade astrocytomas[30]. Moreover, injection of phenotypically wild-type cortical astrocytes and NSC alone fails to elicit tumorigenesis (data not shown). We found that TRP$^{-/-}$ allograft growth exponentially increases 2-3 week post-injection, a time frame during which the proliferative phase of reactive gliosis has ended (**Figures 5** and **7**). To account for potential microenvironmental influences on tumorigenesis upon injection of transformed, nGEM cells into syngeneic mouse brains, particularly during the proliferative phase of reactive gliosis, we recommend performing control injections of phenotypically WT cortical astrocytes or NSC when investigating novel combinations of unrecombined, floxed oncogenic alleles. We also recommend monitoring the

efficiency of tumorigenesis of both phenotypically WT and transformed (recombined) cells at weekly intervals during the first month post-injection, as we have previously described[30].

Through genetic manipulation of either the injected cells or the allograft host itself, the nGEM astrocytoma model system can be used to model many aspects of astrocytoma pathogenesis, including tumor-stroma interactions. As an example, we engineered TRP$^{-/-}$ cortical astrocytes to express luciferase to define tumor growth kinetics *in vivo* (**Figure 7**). Alternatively, nGEM cells could be genetically modified to express a fluorescent protein and orthotopically injected into the brains of GEM with fluorescently labeled neurons or vasculature to define the interactions between tumor cells and normal brain cells[54]. The microenvironmental influence of brain region or developmental age on gliomagenesis can be determined by orthotopically injecting nGEM cells in different locations or in different aged mice. Although short tumor latencies and survival is beneficial for preclinical drug testing, rapid tumor development may not be ideal to model some aspects of astrocytoma pathogenesis, including malignant progression, invasion, and tumor-stoma interactions. Survival of nGEM allograft hosts can be readily manipulated by altering the number of cells injected and systematically monitoring tumor penetrance and latency[30].

Human astrocytomas are genomically complex and exhibit extensive intra and inter-tumor heterogeneity[5-7,55,56]. Potential sources of this heterogeneity include the somatic mutations that initiate tumorigenesis, the mutations acquired during the evolutionary process of malignant progression, and the developmental potential of the cells in which these mutations occur. Large scale sequencing projects have identified many astrocytoma-associated mutations and their patterns of co-occurrence[7]. These studies have relied upon bioinformatic algorithms to identify frequently occurring mutations and to nominate mutations that are likely oncogenic, *i.e.* “driver mutations” that initiate tumorigenesis or drive malignant progression. However, the oncogenic potential of many of these mutations, and their potential cell type specificity, has not been systematically investigated in model systems. We propose that nGEM models utilizing cortical astrocytes and NSC as described here, as well as other neural cell types that can be purified and grown in culture, provide a versatile system to perform such investigations. The sufficiency and necessity for transformation of novel candidate mutations identified through large scale sequencing projects can then be systematically investigated using conventional genetic gain- and loss-of-function approaches with specific nGEM cell types harboring common co-occurring mutations in core GBM pathways for which conditional GEM exist[5]. We further propose that panels of nGEM harboring diverse combinations of mutations in multiple neural cell types will be useful in modeling the genomic heterogeneity of human astrocytomas. Additionally, nGEM astrocytoma models with cortical astrocytes and NSC derived from conditional GEM may provide a tractable model for preclinical drug development because initial *in vitro* testing of both mono- and combination therapies can be performed in these cells to direct more efficient *in vivo* drug testing in immune competent, syngeneic mice. Moreover, immune modulating and stroma-targeted therapies can be tested in nGEM astrocytoma models with immune competent, syngeneic allograft hosts. Thus, nGEM astrocytoma models with transformed cortical astrocytes and NSC are a valuable model system to determine the functional consequences of combinations of oncogenic mutations in specific cell types and may be useful in preclinical drug testing.

Disclosures

The authors have nothing to disclose.

Acknowledgements

CRM is a Damon Runyon-Genentech Clinical Investigator. This work was supported, in part, by grants to CRM from the Damon Runyon Cancer Research Foundation (CI-45-09), Department of Defense (W81XWH-09-2-0042), and University of North Carolina University Cancer Research Fund (UCRF). The authors wish to thank Daniel Roth for mouse husbandry assistance. The authors also wish to thank Hannah Chae, Carter McCormick, Demi Canoutas, Stephanie Gillette, and Susannah Krom for tissue culture and immunofluorescence assistance.

References

1. Dolecek, T. A., Propp, J. M., Stroup, N. E., & Kruchko, C. CBTRUS statistical report: primary brain and central nervous system tumors diagnosed in the United States in 2005-2009. *Neuro Oncol.* **14 Suppl 5**, v1-49, doi:10.1093/neuonc/nos218 (2012).
2. Stupp, R. *et al.* Radiotherapy plus concomitant and adjuvant temozolomide for glioblastoma. *N. Engl. J. Med.* **352** (10), 987-996, doi:10.1056/NEJMoa043330 (2005).
3. Giese, A., Bjerkvig, R., Berens, M. E., & Westphal, M. Cost of migration: invasion of malignant gliomas and implications for treatment. *J. Clin. Oncol.* **21** (8), 1624-1636, doi:10.1200/JCO.2003.05.063 (2003).
4. Miller, C. R., & Perry, A. Glioblastoma. *Arch. Pathol. Lab. Med.* **131** (3), 397-406, doi:10.1043/1543-2165(2007)131[397:G]2.0.CO;2 (2007).
5. Cancer Genome Atlas Research Network. Comprehensive genomic characterization defines human glioblastoma genes and core pathways. *Nature.* **455** (7216), 1061-1068, doi:10.1038/nature07385 (2008).
6. Verhaak, R. G. *et al.* Integrated genomic analysis identifies clinically relevant subtypes of glioblastoma characterized by abnormalities in PDGFRA, IDH1, EGFR, and NF1. *Cancer Cell.* **17** (1), 98-110, doi:10.1016/j.ccr.2009.12.020 (2010).
7. Brennan, C. W. *et al.* The somatic genomic landscape of glioblastoma. *Cell.* **155** (2), 462-477, doi:10.1016/j.cell.2013.09.034 (2013).
8. Phillips, H. S. *et al.* Molecular subclasses of high-grade glioma predict prognosis, delineate a pattern of disease progression, and resemble stages in neurogenesis. *Cancer Cell.* **9** (3), 157-173, doi:10.1016/j.ccr.2006.02.019 (2006).
9. Vitucci, M., Hayes, D. N., & Miller, C. R. Gene expression profiling of gliomas: merging genomic and histopathological classification for personalised therapy. *Br. J. Cancer.* **104** (4), 545-553, doi:10.1038/sj.bjc.6606031 (2011).
10. Sharpless, N. E., & Depinho, R. A. The mighty mouse: genetically engineered mouse models in cancer drug development. *Nat. Rev. Drug Discov.* **5** (9), 741-754, doi:10.1038/nrd2110 (2006).
11. Schmid, R. S., Vitucci, M., & Miller, C. R. Genetically engineered mouse models of diffuse gliomas. *Brain Res. Bull.* **88** (1), 72-79, doi:10.1016/j.brainresbull.2011.06.002 (2012).
12. Siolas, D., & Hannon, G. J. Patient-derived tumor xenografts: transforming clinical samples into mouse models. *Cancer Res.* **73** (17), 5315-5319, doi:10.1158/0008-5472.CAN-13-1069 (2013).

13. Sonoda, Y. *et al.* Formation of intracranial tumors by genetically modified human astrocytes defines four pathways critical in the development of human anaplastic astrocytoma. *Cancer Res.* **61** (13), 4956-4960 (2001).
14. Mao, X. G. *et al.* LIN28A facilitates the transformation of human neural stem cells and promotes glioblastoma tumorigenesis through a pro-invasive genetic program. *Oncotarget.* **4** (7), 1050-1064 (2013).
15. Heyer, J., Kwong, L. N., Lowe, S. W., & Chin, L. Non-germline genetically engineered mouse models for translational cancer research. *Nat. Rev. Cancer.* **10** (7), 470-480, doi:10.1038/nrc2877 (2010).
16. Miller, C. R., Williams, C. R., Buchsbaum, D. J., & Gillespie, G. Y. Intratumoral 5-fluorouracil produced by cytosine deaminase/5-fluorocytosine gene therapy is effective for experimental human glioblastomas. *Cancer Res.* **62** (3), 773-780 (2002).
17. Becher, O. J., & Holland, E. C. Genetically engineered models have advantages over xenografts for preclinical studies. *Cancer Res.* **66** (7), 3355-3358, discussion 3358-3359, doi:10.1158/0008-5472.CAN-05-3827 (2006).
18. Huse, J. T., & Holland, E. C. Genetically engineered mouse models of brain cancer and the promise of preclinical testing. *Brain Pathol.* **19** (1), 132-143, doi:10.1111/j.1750-3639.2008.00234.x (2009).
19. Lee, J. *et al.* Tumor stem cells derived from glioblastomas cultured in bFGF and EGF more closely mirror the phenotype and genotype of primary tumors than do serum-cultured cell lines. *Cancer Cell.* **9** (5), 391-403, doi:10.1016/j.ccr.2006.03.030 (2006).
20. Li, A. *et al.* Genomic changes and gene expression profiles reveal that established glioma cell lines are poorly representative of primary human gliomas. *Mol. Cancer Res.* **6** (1), 21-30, doi:10.1158/1541-7786.MCR-07-0280 (2008).
21. Vries, N. A., Beijnen, J. H., & van Tellingen, O. High-grade glioma mouse models and their applicability for preclinical testing. *Cancer Treat. Rev.* **35** (8), 714-723, doi:10.1016/j.ctrv.2009.08.011 (2009).
22. Clark, M. J. *et al.* U87MG decoded: the genomic sequence of a cytogenetically aberrant human cancer cell line. *PLoS Genet.* **6** (1), e1000832, doi:10.1371/journal.pgen.1000832 (2010).
23. Carvalho, A. C. *et al.* Gliosarcoma stem cells undergo glial and mesenchymal differentiation *in vivo*. *Stem Cells.* **28** (2), 181-190, doi:10.1002/stem.264 (2010).
24. Yost, S. E. *et al.* High-resolution mutational profiling suggests the genetic validity of glioblastoma patient-derived pre-clinical models. *PLoS One.* **8** (2), e56185, doi:10.1371/journal.pone.0056185 (2013).
25. Giannini, C. *et al.* Patient tumor EGFR and PDGFRA gene amplifications retained in an invasive intracranial xenograft model of glioblastoma multiforme. *Neuro Oncol.* **7** (2), 164-176, doi:10.1215/S1152851704000821 (2005).
26. Rich, J. N., Guo, C., McLendon, R. E., Bigner, D. D., Wang, X. F., & Counter, C. M. A genetically tractable model of human glioma formation. *Cancer Res.* **61** (9), 3556-3560 (2001).
27. Chow, L. M. *et al.* Cooperativity within and among Pten, p53, and Rb pathways induces high-grade astrocytoma in adult brain. *Cancer Cell.* **19** (3), 305-316, doi:10.1016/j.ccr.2011.01.039 (2011).
28. Song, Y. *et al.* Evolutionary etiology of high-grade astrocytomas. *Proc. Natl. Acad. Sci. U.S.A.*, doi:10.1073/pnas.1317026110 (2013).
29. Werder, A., Seidler, B., Schmid, R. M., Schneider, G., & Saur, D. Production of avian retroviruses and tissue-specific somatic retroviral gene transfer *in vivo* using the RCAS/TVA system. *Nat. Protoc.* **7** (6), 1167-1183, doi:10.1038/nprot.2012.060 (2012).
30. Vitucci, M. *et al.* Cooperativity between MAPK and PI3K signaling activation is required for glioblastoma pathogenesis. *Neuro Oncol.* **15** (10), 1317-1329, doi:10.1093/neuonc/not084 (2013).
31. Yahanda, A. M., Bruner, J. M., Donehower, L. A., & Morrison, R. S. Astrocytes derived from p53-deficient mice provide a multistep *in vitro* model for development of malignant gliomas. *Mol. Cell. Biol.* **15** (8), 4249-4259 (1995).
32. McEllin, B. *et al.* PTEN loss compromises homologous recombination repair in astrocytes: implications for glioblastoma therapy with temozolomide or poly(ADP-ribose) polymerase inhibitors. *Cancer Res.* **70** (13), 5457-5464, doi:10.1158/0008-5472.CAN-09-4295 (2010).
33. Kim, H. S. *et al.* Gliomagenesis arising from Pten- and Ink4a/Arf-deficient neural progenitor cells is mediated by the p53-Fbxw7/Cdc4 pathway, which controls c-Myc. *Cancer Res.* **72** (22), 6065-6075, doi:10.1158/0008-5472.CAN-12-2594 (2012).
34. Radke, J., Bortolussi, G., & Pagenstecher, A. Akt and c-Myc induce stem-cell markers in mature primary p53(-)/(-) astrocytes and render these cells gliomagenic in the brain of immunocompetent mice. *PLoS One.* **8** (2), e56691, doi:10.1371/journal.pone.0056691 (2013).
35. Marino, S., Vooijs, M., van Der Gulden, H., Jonkers, J., & Berns, A. Induction of medulloblastomas in p53-null mutant mice by somatic inactivation of Rb in the external granular layer cells of the cerebellum. *Genes Dev.* **14** (8), 994-1004 (2000).
36. Zhu, Y. *et al.* Ablation of NF1 function in neurons induces abnormal development of cerebral cortex and reactive gliosis in the brain. *Genes Dev.* **15** (7), 859-876, doi:10.1101/gad.862101 (2001).
37. Jackson, E. L. *et al.* Analysis of lung tumor initiation and progression using conditional expression of oncogenic K-ras. *Genes Dev.* **15** (24), 3243-3248, doi:10.1101/gad.943001 (2001).
38. Xiao, A., Wu, H., Pandolfi, P. P., Louis, D. N., & Van Dyke, T. Astrocyte inactivation of the pRb pathway predisposes mice to malignant astrocytoma development that is accelerated by PTEN mutation. *Cancer Cell.* **1** (2), 157-168 (2002).
39. Xiao, A., Yin, C., Yang, C., Di Cristofano, A., Pandolfi, P. P., & Van Dyke, T. Somatic induction of Pten loss in a preclinical astrocytoma model reveals major roles in disease progression and avenues for target discovery and validation. *Cancer Res.* **65** (12), 5172-5180, doi:10.1158/0008-5472.CAN-04-3902 (2005).
40. Neill, K., Lyons, S. K., Gallagher, W. M., Curran, K. M., & Byrne, A. T. Bioluminescent imaging: a critical tool in pre-clinical oncology research. *J. Pathol.* **220** (3), 317-327, doi:10.1002/path.2656 (2010).
41. McCarthy, K. D., & de Vellis, J. Preparation of separate astroglial and oligodendroglial cell cultures from rat cerebral tissue. *J. Cell Biol.* **85** (3), 890-902 (1980).
42. Azari, H., Sharififar, S., Rahman, M., Ansari, S., & Reynolds, B. A. Establishing embryonic mouse neural stem cell culture using the neurosphere assay. *J. Vis. Exp.* (47), e2457, doi:10.3791/2457 (2011).
43. Giulian, D., & Baker, T. J. Characterization of ameboid microglia isolated from developing mammalian brain. *J. Neurosci.* **6** (8), 2163-2178 (1986).
44. Franken, N. A., Rodermond, H. M., Stap, J., Haveman, J., & van Bree, C. Clonogenic assay of cells *in vitro*. *Nat. Protoc.* **1** (5), 2315-2319, doi:10.1038/nprot.2006.339 (2006).
45. Miller, C. R., Bash, R. E., Vitucci, M., & White, K. K. A genetically-defined, orthotopic allograft model system of glioblastoma: Pathological features and experimental therapeutics. *J. Neuropathol. Exp. Neurol.* **69** (5), 522 (2011).
46. Bash, R. *et al.* Concurrent temozolomide-external beam radiation therapy is effective for experimental glioblastomas in an orthotopic, genetically engineered syngeneic mouse allograft model system. *Neuro Oncol.* **11** (5), 638 (2009).
47. Hamby, M. E., Uliasz, T. F., Hewett, S. J., & Hewett, J. A. Characterization of an improved procedure for the removal of microglia from confluent monolayers of primary astrocytes. *J. Neurosci. Meth.* **150** (1), 128-137, doi:10.1016/j.jneumeth.2005.06.016 (2006).

48. Cahoy, J. D. *et al.* A transcriptome database for astrocytes, neurons, and oligodendrocytes: a new resource for understanding brain development and function. *J. Neurosci.* **28** (1), 264-278, doi:10.1523/JNEUROSCI.4178-07.2008 (2008).
49. Foo, L. C. *et al.* Development of a method for the purification and culture of rodent astrocytes. *Neuron.* **71** (5), 799-811, doi:10.1016/j.neuron.2011.07.022 (2011).
50. Rietze, R. L., Valcanis, H., Brooker, G. F., Thomas, T., Voss, A. K., & Bartlett, P. F. Purification of a pluripotent neural stem cell from the adult mouse brain. *Nature.* **412** (6848), 736-739, doi:10.1038/35089085 (2001).
51. Campisi, J. Aging, cellular senescence, and cancer. *Annu. Rev. Physiol.* **75**, 685-705, doi:10.1146/annurev-physiol-030212-183653 (2013).
52. Sirko, S. *et al.* Reactive glia in the injured brain acquire stem cell properties in response to sonic hedgehog. *Cell stem cell.* **12** (4), 426-439, doi:10.1016/j.stem.2013.01.019 (2013).
53. Robel, S., Berninger, B., & Gotz, M. The stem cell potential of glia: lessons from reactive gliosis. *Nat. Rev. Neurosci.* **12** (2), 88-104, doi:10.1038/nrn2978 (2011).
54. Burrell, K., Agnihotri, S., Leung, M., Dacosta, R., Hill, R., & Zadeh, G. A novel high-resolution *in vivo* imaging technique to study the dynamic response of intracranial structures to tumor growth and therapeutics. *J. Vis. Exp.* (76), e50363, doi:10.3791/50363 (2013).
55. Sottoriva, A. *et al.* Intratumor heterogeneity in human glioblastoma reflects cancer evolutionary dynamics. *Proc. Natl. Acad. Sci. U.S.A.* **110** (10), 4009-4014, doi:10.1073/pnas.1219747110 (2013).
56. Snuderl, M. *et al.* Mosaic amplification of multiple receptor tyrosine kinase genes in glioblastoma. *Cancer Cell.* **20** (6), 810-817, doi:10.1016/j.ccr.2011.11.005 (2011).

